JOURNAL OF SOLID STATE CHEMISTRY **129,** 184–188 (1997)
ARTICLE NO. SC967204

Synthesis, Structure, and Properties of the Noncentrosymmetric Pyroborate $BaCuB_2O_5$

Robert W. Smith

Department of Physics, University of Nebraska at Omaha, Omaha, Nebraska 68182-0266

and

Douglas A. Keszler

Department of Chemistry and Center for Advanced Materials Research, Oregon State University, Gilbert Hall 153, Corvallis, Oregon 97331-4003

Received October 23 1995; in revised form October 22, 1996; accepted October 24, 1996

The new noncentrosymmetric pyroborate $BaCuB_2O_5$ has been synthesized and its structure determined by single-crystal X-ray methods. It crystallizes in the monoclinic space group C2 with a cell of dimensions $a=6.485(1)$, $b=9.165(1)$, $c=3.971(1)$ Å, and $\beta=96.14(1)^\circ$. The structure was determined from 1281 unique reflections and refined to the final residuals $R=0.039$ and $wR=0.049$. It is composed of highly distorted $[CuO_4]$ squares and double-triangular $[B_2O_5]$ groups that are connected to form infinite two-dimensional layers. The layers are stacked parallel to (001), and the Ba atoms interleave successive layers. Parallel alignment of the pyroborate groups is conductive to high efficiency for optical frequency conversion. The magnetic moment at 22°C is $1.69 \pm 0.03\ \mu_B$. © 1997 Academic Press

INTRODUCTION

Solid-state borates exhibit a variety of physical and chemical features, ranging from nonlinear optical properties (1) to the catalytic activity of the copper borate $Cu_2Al_6B_4O_{17}$ (2). As part of an effort to synthesize new examples, we have investigated the BaO–CuO–B_2O_3 phase diagram. In this report, we describe the synthesis, structure, and properties of the new, noncentrosymmetric material $BaCuB_2O_5$.

EXPERIMENTAL

Synthesis and Crystal Growth

The title compound was prepared by grinding a stoichiometric ratio of $Ba(NO_3)_2$ (reagent grade, Mallinckrodt), $Cu(NO_3)_2 \cdot 2\frac{1}{2}H_2O$ (reagent grade, Mallinckrodt), and B_2O_3 (99.99%, Morton Thiokol) under hexane to a fine powder and heating at 600°C for 30 min in a Pt crucible. The mixture was then heated at 800°C for a total of 18 h with several grindings between heatings. The sample was single phase as determined by analysis of the X-ray pattern obtained from an automated Philips powder diffractometer equipped with graphite-monochromated Cu$K\alpha$ radiation.

Single crystals were grown from a melt containing a PbO flux. A mixture in the solute:flux ratio of 4:1 by mass was heated in a Pt crucible to 1203 K, cooled at 6 K/h to 873 K, and then quenched to room temperature. A transparent, green single crystal of dimensions $0.24 \times 0.14 \times 0.08$ mm was physically separated from the crucible for structure analysis.

X-Ray Work

Single-crystal X-ray measurements were done on a Rigaku AFC6R diffractometer equipped with monochromatic Mo$K\alpha$ radiation. Lattice parameters were refined from 15 reflections in the range $35^\circ < 2\theta < 43^\circ$. Intensity data in the range $0 \le h \le 14$, $0 \le k \le 20$, and $-9 \le l \le 9$ were collected with the ω-2θ scan technique at a scan speed of 16°/min in ω and a scan width $\Delta\omega = (1.55 + 0.3 \tan\theta)^\circ$. The intensities of three standard reflections were measured after each block of 300 data and found to vary by less than 3%. From 1349 reflections measured to $2\theta = 100^\circ$, 1281 unique data having $F_0^2 \ge 3\sigma(F_0^2)$ were obtained.

All calculations for structure solution and refinement were performed on a micro Vax II computer with programs from the TEXSAN crystallographic software package (3). Three space groups are consistent with the systematic absences hkl, $h + k = 2n + l$, and $h0l$, $h = 2n + l$, noncentrosymmetric $C2$ or Cm and centrosymmetric $C2/m$. Results from second harmonic generation (SHG) experiments (*vide infra*) and the statistical distribution of intensities (4) indicate that the structure is noncentrosymmetric. We favor the space group $C2$ (No. 5) on basis of the successful solution and refinement of the structure in this group; it is the only group that provides satisfactory positions for the light

0022-4596/97 $25.00
Copyright © 1997 by Academic Press
All rights of reproduction in any form reserved.

B and O atoms. The complete absence of a mirror plane of symmetry in the resulting solution is also consistent with the favored group.

The positional parameters for the Ba and Cu atoms were found with the direct-methods program MITHRIL (5), and the remaining atomic coordinates were determined from analysis of difference electron density maps. Following refinement with isotropic displacement parameters, the data were corrected for absorption with the computer program DIFABS (6). Final least-squares refinement on F_0 with data having $F_0^2 \geq 3\sigma(F_0^2)$ and anisotropic displacement factors for each atom resulted in the residuals $R(F) = 0.039$ and $wR(F) = 0.049$ $[w = 1/\sigma^2(F)]$; neutral atomic scattering factors were taken frm the usual source (7). The largest peak in the final difference map has a height of 0.91% of the Ba atom. Additional crystal data and experimental conditions are summarized in Table 1, and final atomic parameters are listed in Table 2.

Unit-cell parameters were also obtained from powder X-ray data by least-squares refinement of 2θ values. A powder sample was ground, sieved with a 100-mesh wire screen, and then annealed at 973 K for 2 h. The 2θ values of 14 intense reflections in the range $26^\circ < 2\theta < 56^\circ$ were determined and corrected by using Si (NIST Standard Reference Material 640b) as the internal standard. The refind cell parameters $a = 6.485(2)$, $b = 9.170(3)$, $c = 3.974(1)$ Å, and $\beta = 96.11(3)^\circ$ compare well to the results obtained from the single-crystal data (*cf.* Table I).

Magnetic Moment

The effective magnetic moment was obtained at 295 K by the Guoy method. Measurements were made at a field strength of 5 kG by using an Alpha Model AL 7500 water-cooled magnet with 4-in. pole faces and a 1.5-in. air gap. The Guoy tube was calibrated with $HgCo(SCN)_4$. Diamagnetic corrections of the molar susceptibility were made from reported values (8).

TABLE 1
Crystal Data and Experimental Conditions for $BaCuB_2O_5$

Diffractometer	Rigaku AFC6R
Radiation	Mo$K\alpha$
λ, Å	0.70926
Formula wt., amu	302.49
a, Å	6.485(1)
b, Å	9.165(1)
c, Å	3.971(5)
β, °	96.14(1)
V, Å^3	234.68(8)
Space group	$C2$
ρ_{calc}, g cm^{-3}	4.28
Crystal vol., mm^3	0.0027
F (000)	270
Z	2
Linear abs. coeff., cm^{-1}	128.10
p factor	0.05
T, K	296
No. unique data with $F_0^2 \geqslant 3\sigma(F_0^2)$	1281
$R(F_0)$	0.039
$wR(F_0)$	0.049

TABLE 2
Final Atomic Coordinates and Displacement Factors for $BaCuB_2O_5$

Atom	Wyckoff notation	x	y	z	B_{eq}[a]
Ba	2(a)	0	0	0	0.641(7)
Cu	2(b)	0	0.5898(1)	1/2	0.79(2)
B	4(c)	0.1792(7)	0.3087(5)	0.40(1)	0.6(1)
O1	2(b)	0	0.2380(6)	1/2	1.0(1)
O2	4(c)	0.2137(5)	0.4529(4)	0.465(1)	0.8(1)
O3	4(c)	0.3132(6)	0.2279(4)	0.243(1)	1.0(1)

Second Harmonic Generation

A measurement of the SHG efficiency was obtained with a pulsed Nd:YAG laser operating at 1064 nm. Several dozen crystallites (< 0.1 mm on edge) were placed on a fused silica plate inside the sample cell. Visible light was filtered from the laser beam with a Corning 1-75 filter having a transmittance of 87% at 1064 nm and $< 1\%$ at 532 nm. IR radiation was filtered from the output with a Corning 7-57 filter having a transmittance of 88% at 532 nm and 1% at 1064 nm. The second-harmonic signal was monitored with a photomultiplier attached to an oscilloscope. SHG measurements of potassium dihydrogen phosphate (KDP) crystallites served as a standard for the measurement; the KDP measurements were made before and after data acquisition from the sample of $BaCuB_2O_5$ crystals.

RESULTS AND DISCUSSION

Structure

A labeled drawing of the contents of the unit cell is shown in Fig. 1, and selected bond distances and angles are listed in Table 3.

The structure is a new type that is best described as containing infinite two-dimensional sheets of fused $[B_2O_5]$ double triangles and highly distorted $[CuO_4]$ squares that extend parallel to the plane (001); Ba atoms interleave successive sheets. A portion of this infinite two-dimensional copper pyroborate layer is shown in Fig. 2. Each $[CuO_4]$ square is connected to three $[B_2O_5]$ groups. In one of these connections, the $[B_2O_5]$ group binds in a bidentate manner through two *cis* O2 atoms of the Cu-centered polyhedron, while the other groups share vertices with the square through one O3 atom each. Hollows bordered by O atoms

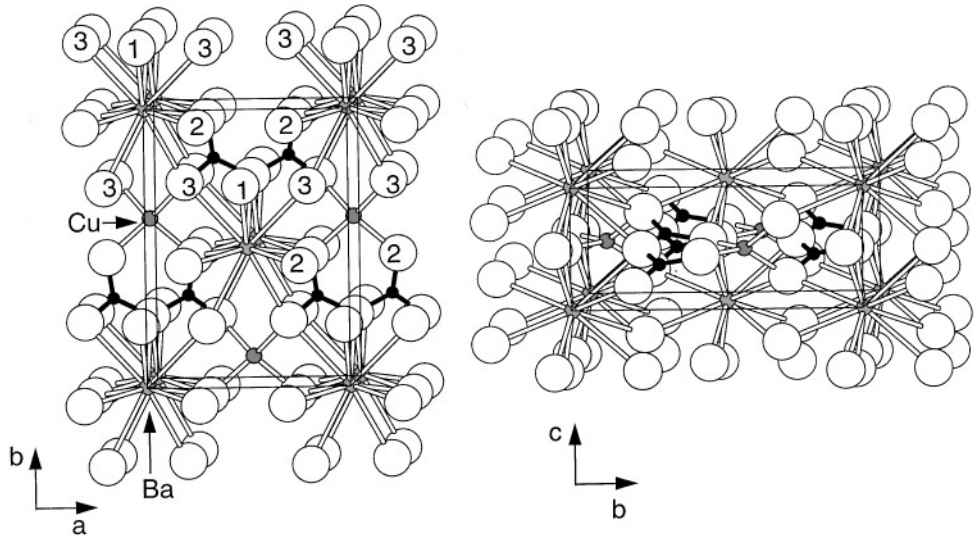

FIG. 1. Labeled sketch of the unit cell viewed (left) along the *c* axis and (right) along the *a* axis. Large numbered circles represent O atoms, and small filled circles represent B atoms.

are present in each layer, and the Ba atoms occupy sites above and below these nooks.

A structure similar to $BaCuB_2O_5$ is realized with the noncentrosymmetric pyroborates $ANbOB_2O_5$ (where A = Cs (9a), Rb (9b), and K (9c)). These compounds contain niobium pyroborate layers that are topologically similar to the copper pyroborate layers of $BaCuB_2O_5$. The $ANbOB_2O_5$ compounds, however, have additional O atoms *between* the layers that bind to the intralayer Nb atoms. Consequently, the Nb atoms in $ANbOB_2O_5$ occupy distorted octahedral O environments rather than the distorted squares of the Cu atoms in $BaCuB_2O_5$.

TABLE 3
Selected Interatomic Distances (Å) and Angles (°) for $BaCuB_2O_5$

Atoms	Distance	Atoms	Angle
Ba–O2	2.703(4) × 2	02–Ba–O2	161.6(1)
Ba–O2	2.788(4) × 2	O2–Ba–O2	162.2(1)
Ba–O1	2.950(4) × 2	O1–Ba–O1	84.6(1)
Ba–O3	2.980(4) × 2	O3–Ba–O3	66.4(1)
Ba–O3	2.996(4) × 2	O3–Ba–O3	91.6(1)
		O1–Ba–O3	46.9(1)
		O1–Ba–O3	69.6(1)
		O1–Ba–O2	68.8(1)
		O1–Ba–O2	67.7(1)
		O2–Ba–O3	81.4(1)
		O2–Ba–O3	48.1(1)
		O2–Ba–O3	58.3(1)
		O2–Ba–O3	81.1(1)
Cu–O2	1.885(3) × 2	O2–Cu–O2	96.6(2)
Cu–O3	1.965(4) × 2	O3–Cu–O3	99.8(3)
		O2–Cu–O3	92.7(2)
		O2–Cu–O3	114.0(2)
B–O3	1.345(6)	O3–B–O2	121.4(4)
B–O2	1.359(5)	O2–B–O1	121.0(4)
B–O1	1.422(5)	O1–B–O3	117.6(4)

The copper pyroborate layer in $BaCuB_2O_5$ exhibits considerable deviations from planarity. The $[CuO_4]$ squares (Fig. 2) are tetrahedrally distorted; each pair of O3 vertices is positioned above or below the plane containing the Cu and O2 atoms. This is illustrated by the O2–Cu–O3 angle of 144.0(2)° and the four other O–Cu–O angles with values ranging from 92.7(2) to 98.8(3)°. Cu–O bond lengths average 1.93 ± 0.05 Å and are comparable to bond distances reported for other copper borates, e.g., 1.94 ± 0.01 Å in $SrCu_2(BO_3)_2$ (10), 1.930 ± 0.006 and 1.94 ± 0.04 Å in α- and β-$Sr_2Cu(BO_3)_2$, respectively (11), and 1.95 ± 0.04 Å in $Ba_2Cu(BO_3)_2$ (12).

Typical structural characteristics are also displayed by the pyroborate anion. The B–O1–B angle is 125.8(5)°, and the two triangles deviate from planarity by approximately 8°. These values fall within the reported ranges of B–O–B angles, 112°–180°, and interplanar angles, 0°–76.8° (13). As previously noted (13), the geometry of the $[B_2O_5]$ group is primarily dictated by packing constraints and the nature of the associated cations in a given structure. The B–O1 bond is also significantly longer than the other two B–O bonds (1.422 ± 0.005 Å vs 1.35 ± 0.01 Å). Atom O1 binds to two B atoms, whereas atoms O2 and O3 bind to only one B atom each. Thus, the available σ electron density on atom O1 is dispersed through two covalent B–O interactions, weakening the B–O1 bonds and increasing their length.

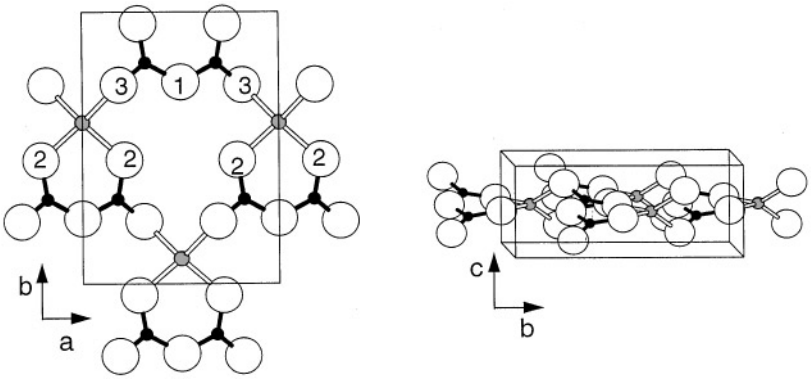

FIG. 2. Sketch of a portion of the copper pyroborate network viewed (left) along [001] and (right) along [100].

Ten O atoms form bonds to each Ba atom, five from each copper pyroborate sheet. The Ba coordination may be described as a distorted bicapped, square antiprism with the Ba atom resting nearer the distorted square of four O2 atoms than to the square of two O1 and two O3 atoms (*cf.* Scheme 1). The average Ba–O distance, 2.88 ± 0.09 Å, compares well to the expected value of 2.90 Å calculated from the crystal radii for a 10-coordinate Ba^{2+} ion and a 4-coordinate O^{2-} ion (14). All O atoms are coordinated by four metal atoms, occupying distorted tetrahedra.

Magnetic Moment

The effective magnetic moment at 295 K is 1.69 ± 0.03 μ_B. This value is consistent with the d^9 electron configuration of the Cu^{2+} ion and spin-only contributions to the magnetic moment. Values typically range from 1.7 to 1.9 μ_B for copper(II) complexes (15) and average 1.63 μ_B in $ACuO_2$ where A = Ca, Sr, or Ba (16).

SHG

The second-harmonic signal of $BaCuB_2O_5$ is 14% of that in KDP. While the SHG signal provides further evidence that the compund crystallizes in a noncentrosymmetric space group, the observed magnitude is weaker than would be anticipated from the alignment and density of the B_2O_5 chromophores. Of course, the presence of the d^9, Cu^{2+} ions in the compound is expected to have a significant effect on the SHG properties. The unpaired *d* electron likely undergoes electronic transitions that result in some absorption in the frequency range of the second harmonic of the Nd:YAG laser; the crystals have a blue–green color.

Compounds that crystallize in space group *C*2 have a permanent dipole moment directed along the *b* axis. Since the distorted pyroborate groups are mostly directed along this axis, they will contribute to the dipole moment and significantly to the nonlinear optical susceptibility. The highly distorted [CuO_4] squares should also contribute, considering the 0.08-Å difference between the Cu–O2 and Cu–O3 interatomic distances. In addition, reported data indicate that the structurally related compound $KNbOB_2O_5$ has a d_{eff} for SHG that is approximately five times that of KDP (9c). If it is assumed that the pyroborate group makes the principal contribution to d_{eff}, the parallel orientation of these groups in the present structure should result in a significant SHG effect.

Attempts have been made to produce a colorless derivative by eliminating the absorption bands in the visible portion of the spectrum associated with the Cu^{2+} ion through replacement of said ion with Zn^{2+}. In the BaO-ZuO-B_2O_3 phase diagram, however, only two borates have been identified, i.e., $BaZn_2(BO_3)_2$ (17) and $Ba_2Zn(BO_3)_2$ (18).

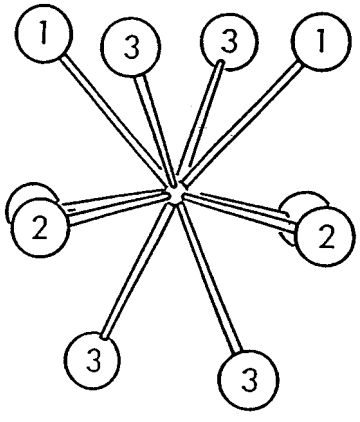

SCHEME 1

ACKNOWLEDGMENTS

We thank Professor Joseph Nibler of Oregon State University for his assistance with the SHG measurement. Funds for this research were provided by the National Science Foundation, Solid-State Chemistry Program. D.A.K. thanks the Alfred P. Sloan Foundation for a research fellowship.

REFERENCES

1. C. T. Chen and G. Z. Liu, *Ann. Rev. Mater. Sci.* **16,** 203 (1986); D. A. Keszler, A. Akella, K. I. Schaffers, and T. Alekel III, *Mater. Res. Soc. Symp. Proc.* **329,** 15 (1994).
2. A. Zletz (Amoco Corp.), U.S. Patent Application 709, 790, 11 March 1985.
3. Molecular Structure Corporation, "TEXSAN," 3200A Research Forest Drive, The Woodlands, TX 77381, 1985.
4. E. R. Howells, D. C. Phillips, and D. Rogers, *Acta Crystallogr.* **3,** 210 (1950).
5. G. J. Gilmore, "MITHRIL: A Computer Program for the Automatic Solution of Crystal Structures from X-ray Data," University of Glasgow, Scotland, 1983.
6. N. Walker and D. Stuart, *Acta Crystallogr. Sect A* **39,** 158 (1983).
7. D. T. Cromer and J. T. Waber, *in* "International Tables for X-ray Crystallography," Vol IV, Table 2.2A, p. 71, Kynoch Press, Birmingham, 1974.
8. L. N. Mulay and E. A. Boudreaux, "Theory and Applications of Molecular Diamagnetism," pp. 306–307, Wiley, New York, 1976.
9. (a) D. A. Keszler, A. Akella, K. I. Schaffers, and T. Alekel III, *Mater. Res. Soc. Symp. Proc.* **329,** 15 (1994); A. Akella and D. A. Keszler, *J. Solid State Chem.* **120,** 74 (1995); P. Becker, L. Bohatý and F. Fröhlich, *Acta Crystallogr. Sect. C* **51,** 1721 (1995). (b) A. Baucher, M. Gasperin, B. Cerville, *Acta Crystallogr. Sect. B* **32**, 2211 (1976). (c) J. F. H. Nicolls, B. H. T. Chai, D. L. Corker, J. C. Calabrese, and B. Henderson, *Proc. SPIE – Int. Soc. Opt. Eng.* **1863,** 54 (1993).
10. R. W. Smith and D. A. Keszler, *J. Solid State Chem.* **93,** 430 (1991).
11. R. W. Smith and D. A. Keszler, *J. Solid State Chem.* **81,** 305 (1989).
12. R. W. Smith and D. A. Keszler, *Acta Crystallogr. Sect. C* **46,** 370 (1990).
13. P. D. Thompson, J. Huang, R. W. Smith, and D. A. Keszler, *J. Solid State Chem.* **95,** 126 (1991).
14. R. D. Shannon, *Acta Crystallogr. Sect A* **32,** 751 (1976).
15. E. A. Boudreaux and L. N. Mulay, "Theory and Applications of Molecular Paramagnetism," p. 54, Wiley, New York, 1976.
16. M. Arjomand and D. J. Machin, *J. Chem. Soc. Dalton Trans.* 1061 (1975).
17. R. W. Smith and D. A. Keszler, *J. Solid State Chem.* **100,** 325 (1992).
18. R. W. Smith and L. J. Koliha, *Mater. Res. Bull.* **29,** 1203 (1994).